

# Development of Hybrid Membranes Using Chitosan and Silica Precursors for Pervaporation Separation of Water + Isopropanol Mixtures

Jolly G. Varghese,<sup>†</sup> Ramesh S. Karuppanan,<sup>‡</sup> and Mahadevappa Y. Kariduraganavar<sup>\*,†</sup>

Center of Excellence in Polymer Science and Department of Chemistry, Karnatak University, Dharwad 580 003, India, and Indian Institute of Science, Bangalore 560 012, India

Using a sol–gel technique, organic–inorganic hybrid membranes were prepared using chitosan and mixed silica precursors such as tetraethoxysilane and  $\gamma$ -glycidoxypropyltrimethoxysilane. The  $\gamma$ -glycidoxypropyltrimethoxysilane acted as a coupling agent to enhance the compatibility between the organic (chitosan) and the inorganic (tetraethoxysilane) phase. Different techniques such as Fourier transform infrared spectroscopy (FTIR), wide-angle X-ray diffraction (WAXD), scanning electron microscopy (SEM), and thermogravimetric analysis (TGA) were employed to study the physicochemical changes in the resulting membranes. These membranes were tested for their ability to separate water + isopropanol mixtures by pervaporation in the temperature range of (303 to 323) K. The experimental data demonstrated that both flux and selectivity were increased simultaneously with increasing the amount of  $\gamma$ -glycidoxypropyltrimethoxysilane. However, this trend no longer remained when the content of  $\gamma$ -glycidoxypropyltrimethoxysilane was increased beyond 0.25 mass fraction. The membrane containing 0.25 mass fraction of  $\gamma$ -glycidoxypropyltrimethoxysilane (M-2) exhibited the highest separation selectivity of 18 981 with a thickness-normalized flux of  $7.45 \cdot 10^{-7} \text{ kg} \cdot \text{m}^{-1} \cdot \text{h}^{-1}$  at 303 K. The total flux and flux of water were found to be overlapping with up to 0.25 mass fraction of  $\gamma$ -glycidoxypropyltrimethoxysilane, suggesting that these membranes could be used effectively to break the azeotropic point of water–isopropanol mixtures. From the temperature-dependent permeation values, the Arrhenius activation parameters were estimated. The activation energy values obtained for water permeation ( $E_{pw}$ ) are significantly lower than those of isopropanol permeation ( $E_{pIPA}$ ), suggesting that the developed membranes have demonstrated an excellent separation performance for water–isopropanol systems.

## Introduction

Recently, the field of materials science has witnessed the emergence of a novel class of materials called organic–inorganic hybrids.<sup>1,2</sup> These materials are of intense interest in contemporary material chemistry because of their great potential in value-added applications. Until today, numerous hybrid organic–inorganic materials have been developed, providing access to an immense new area in materials science.<sup>1,3–5</sup> The major driving force behind the intense activities in this area are the new and different properties of these materials, which the traditional composites and conventional materials do not have. These multifunctional advanced materials have a major impact on future applications in the fields<sup>3–6</sup> such as optics, electronics, ionics, mechanics, protective coatings, sensors, drug delivery, and membranes.

The development of hybrid organic–inorganic materials is mainly due to the development of the soft inorganic chemistry processes, especially sol–gel processes, where mild synthetic conditions allow versatile access to chemically designed combinations of inorganic domains obtained via inorganic polymerization reactions with fragile entities such as organic or even bioactive molecules.<sup>7–11</sup> The interactions between the organic and the inorganic phases during synthesis can occur at the nano or molecular scale, resulting in nanocomposites with small sizes and large interphases. These interactions in essence result in a

new material with multifunctional properties depending upon the interactions. Thus, the mechanical, chemical, and physical properties of these materials can be tailored by judiciously adjusting the polymer and its concentration and the molecular weight for the desired applications.<sup>12,13</sup> They can easily combine the balanced properties of organic polymers and silica and even can acquire some special or novel properties due to their micro and nanostructures. Consequently, organic–inorganic materials can be potentially used in membrane applications.<sup>14,15</sup>

Considering these aspects, several researchers including our group have prepared organic–inorganic hybrid membranes and studied extensively for pervaporation (PV) separation of aqueous + organic mixtures.<sup>16–22</sup> These hybrid membranes mainly composed of hydrophilic polymers especially polysaccharides such as alginate and chitosan.<sup>23,24</sup> Among these, chitosan has been widely used as a PV membrane material because of its high hydrophilicity, good film-forming ability, and excellent chemical resistant properties.<sup>25,26</sup> The only drawback is that at higher concentrations of water chitosan undergoes excess swelling and loses its mechanical stability and water permselectivity.

To overcome this, many researchers have used tetraethoxysilane (TEOS) as an inorganic precursor to establish the cross-links in the membrane matrix. Unfortunately, the silica network formed from the self-condensation of silanol groups of TEOS led to macroscopic phase separation between silica and the polymer domain due to lack of covalent bonding. In addition, the fast self-condensation reaction rate of TEOS brought some inconveniences to the preparation of hybrid materials. Park et

\* Corresponding author. E-mail: mahadevappak@yahoo.com. Fax: +91-836-2771275. Phone: +91-836-2215286ext. 23.

<sup>†</sup> Karnatak University.

<sup>‡</sup> Indian Institute of Science.

al.<sup>27</sup> used a precondensed TEOS network to blend with chitosan to overcome such a problem. Hsiue et al.<sup>28</sup> employed phenyltriethoxysilane to slow down the condensation rate and to enhance the polymer-silica compatibility. Liu et al.<sup>29</sup> have introduced  $\gamma$ -glycidoxypropyltrimethoxysilane (GPTMS) into chitosan and found the moderate condensation rate of silanol in sol-gel process while effectively preventing the macro-phase separation during the formation of membrane. This is possible because GPTMS has an organically modified alkoxide moiety containing an epoxy ring. The opening of the epoxy ring allows the formation of hydroxyl group, rendering the inorganic sols with higher hydrophilicity and thus better compatibility, to be achieved between the organic and the inorganic phases.<sup>30</sup>

Therefore, the present study addresses the preparation of organic-inorganic hybrid membranes by incorporating mixed silica precursors such as TEOS and GPTMS into chitosan solution. The characterization of the membranes was made using Fourier transform infrared spectroscopy (FTIR), wide-angle X-ray diffraction (WAXD), scanning electron microscopy (SEM), and thermogravimetric analysis (TGA). The coupling agent GPTMS was introduced to increase the compatibility between the organic and the inorganic phases and thereby to inhibit the phase separation. The effect of the relative molar content of GPTMS on the physicochemical properties of the hybrid membranes was studied. The effects of silica precursors and water composition on the PV separation of water-isopropanol mixtures were systematically investigated. From the temperature dependence of permeation flux, the Arrhenius activation parameters were estimated. The results were discussed in terms of PV separation efficiency of the membranes.

## Experimental Section

**Materials.** Chitosan [ $M_w \approx 200\,000$ ;  $N$ -deacetylation degree (75 to 85) %], TEOS, and GPTMS were purchased from Sigma-Aldrich Chemie, GmbH, Germany. Isopropanol (IPA) and acetic acid (HAc) were procured from s.d. Fine Chemicals Ltd., Mumbai, India. All of the chemicals were of reagent grade and used without further purification. Double-distilled water was used throughout the study.

**Membrane Preparation.** Chitosan (3 g) was dissolved in 100 mL of deaerated-distilled water containing 2 volume fraction acetic acid with constant stirring for about 24 h at room temperature. The resulting solution was filtered to remove the undissolved residue particles. To this clear solution, 1 mL of  $0.30\text{ mol}\cdot\text{L}^{-1}$  HCl and 1 g of TEOS were added, and the solution was stirred for 12 h. The resulting solution was cast onto a glass plate with the aid of a casting knife in a dust-free atmosphere at room temperature. After being dried for about 48 h, the membrane was subsequently peeled off and is designated as M-1.

To prepare organic-inorganic hybrid membranes, known weights of GPTMS, (0.25, 0.50, and 0.75) g, were added into TEOS-added chitosan solutions. To maintain the same amount of silica precursors in the chitosan solution, the amount of TEOS was correspondingly reduced to (0.75, 0.50, and 0.25) g, respectively. However, the amount of chitosan was kept constant in all of the solutions. The rest of the procedure was followed as similar to the preparation of membrane M-1, and the membranes thus obtained were designated as M-2, M-3, and M-4, respectively. Before subjected to the PV experiment, the membrane thickness was measured at different points using Peacock dial thickness gauge (model G, sensitivity  $\pm 2\ \mu\text{m}$ , made by Ozaki MFG Co. Ltd., Japan). The thickness of the membranes was found to be  $(40 \pm 2)\ \mu\text{m}$ .

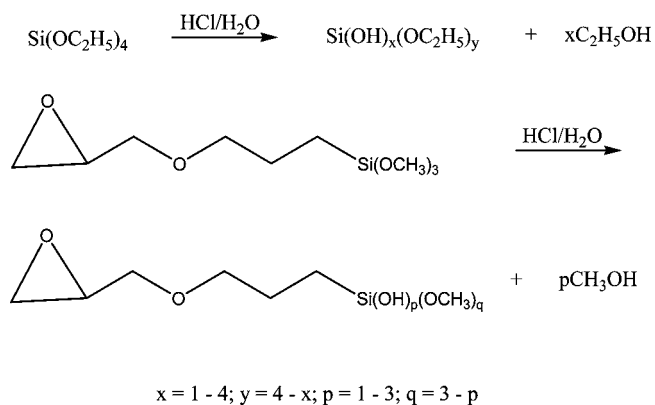


**Figure 1.** Scheme for hydrolysis of TEOS and GPTMS.

**Swelling Measurements.** The dried membrane samples were weighed on a digital microbalance (model B204-S, sensitivity  $\pm 0.01\text{ mg}$ , made by Mettler-Toledo International, Zurich, Switzerland) and immediately immersed in various compositions of water-isopropanol mixtures at a temperature of 303 K for 24 h. The swollen membranes were removed from the sealed vessels, wiped carefully with blotting paper to remove the adhered solvent, and weighed as quickly as possible. All of the experiments were performed at least three times, and the results were averaged. The percent degree of swelling (DS) was calculated as:

$$\text{DS (0.01)} = \left( \frac{M_s - M_d}{M_d} \right) \quad (1)$$

where  $M_s$  and  $M_d$  are the masses of the swollen and dry membranes, respectively.

**Pervaporation Experiments.** PV experiments were performed using the in-house designed apparatus as reported in our previous articles.<sup>21,31</sup> The effective surface area of the membrane in contact with the feed mixture was  $34.23\text{ cm}^2$ , and the capacity of the feed compartment was about  $250\text{ cm}^3$ . The vacuum in the downstream side of the apparatus was maintained ( $1.333224\text{ kPa}$ ) using a two-stage vacuum pump (sensitivity  $\pm 0.065\text{ kPa}$ , made by Toshniwal, Chennai, India). The mass fraction of water in the feed mixture was varied from 0.05 to 0.25. While maintaining the temperature, the test membrane was allowed to equilibrate for about 2 h in the feed compartment with a known volume of feed mixture before performing the PV experiment. After a steady state was attained, the permeate was collected in a trap immersed in the liquid nitrogen jar on the downstream side at fixed intervals of time. The experiments were carried out at (303, 313, and 323) K. The flux was calculated by weighing the permeate on a digital microbalance. The composition of water and isopropanol in the permeate was estimated by measuring the refractive index of the permeate using an Abbe's refractometer (sensitivity  $\pm 0.0001$ , made by Atago-3T, Japan) and by comparing it with a standard graph that was established previously with the known compositions of water-isopropanol mixtures. All of the experiments were performed at least three times, and the results were averaged. The results of permeation for water + isopropanol mixtures during the PV were reproducible within the relative range of  $\pm 0.05$ .

From the PV data, the separation performance of the membranes was assessed in terms of total flux ( $J$ ), separation selectivity ( $\alpha$ ), and PV separation index (PSI). These were respectively calculated using the following equations:

$$J = \frac{M}{At} \quad (2)$$

$$\alpha = \frac{P_w/P_{IPA}}{F_w/F_{IPA}} \quad (3)$$

$$PSI = J(\alpha_{sep} - 1) \quad (4)$$

where  $M$  is the mass of permeate;  $A$ , the effective membrane area;  $t$ , the permeation time;  $P_w$  and  $P_{IPA}$  are the mass fraction of water and isopropanol in the permeate, respectively;  $F_w$  and  $F_{IPA}$  are the respective mass fraction of water and isopropanol in the feed. From the values of flux, we have further calculated

thickness-normalized flux ( $J^* = Jl$ , where  $l$  is the thickness of the membrane).

## Results and Discussion

**Synthesis of Hybrid Membranes.** The reaction mechanism for the synthesis of chitosan–siloxane hybrid membrane is shown in Figures 1 and 2. Prior to the synthesis of hybrid membranes, both GPTMS and TEOS were partially hydrolyzed in the acidic condition, and the resulting hydrolyzed reactants were added to an aqueous chitosan solution to form siloxane. Under the acidic conditions, the epoxy rings of GPTMS opened,

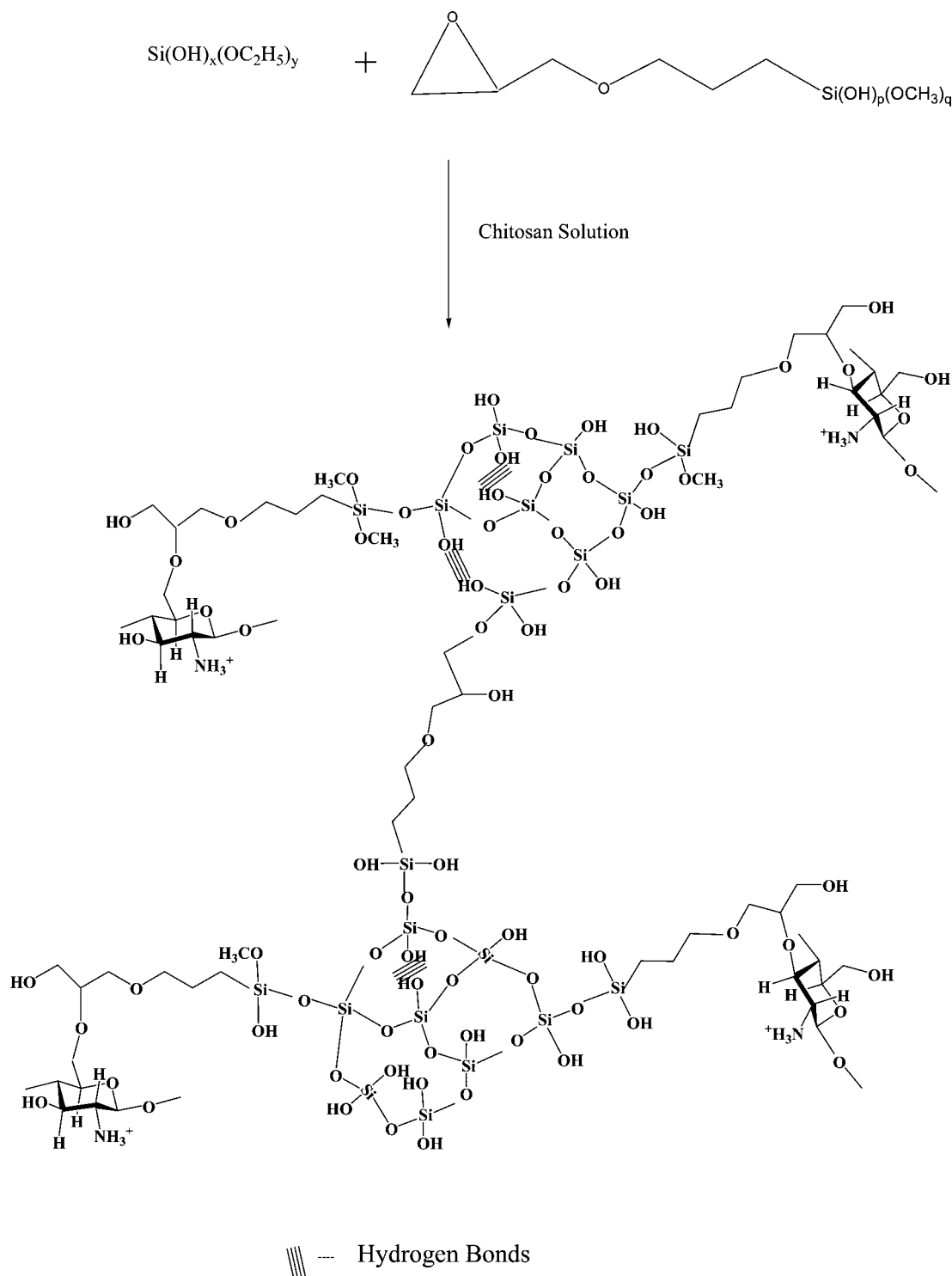
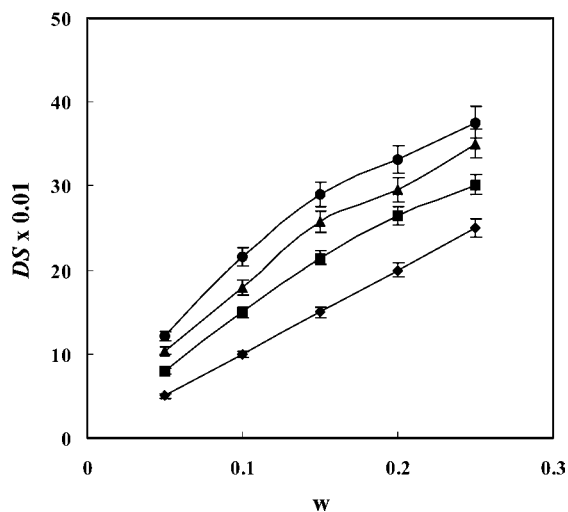


Figure 2. Scheme for the condensation reaction.



**Figure 3.** Variation of degree of swelling (DS) with different mass fractions of water ( $w$ ) in the feed for hybrid membranes:  $\blacklozenge$ , (M-1) 100/0 mass ratio;  $\blacksquare$ , (M-2) 75/25 mass ratio;  $\blacktriangle$ , (M-3) 50/50 mass ratio;  $\bullet$ , (M-4) 25/75 mass ratio of TEOS/GPTMS.

and subsequently reacted with hydroxyl groups of chitosan to form C–O–C bonds. The possibility of reaction with  $-\text{NH}_2$  groups of chitosan was ruled out since all of the  $-\text{NH}_2$  groups were converted into  $-\text{NH}_3^+$  by the addition of acetic acid. During the formation of siloxanes, the co-condensation reaction occurred between the silanols and/or alkoxy silanes by dehydration and/or dealcoholysis. The flexible units arising from GPTMS could bridge between the silica particles and the chitosan chain, which remarkably improved the toughness of the hybrid membranes.

**Effects of Feed Composition and Silica Precursors on Membrane Swelling.** In PV, both permeation flux and selectivity of a membrane are generally dependent on the degree of membrane swelling, which occurs as a result of the interactions between the membrane and the contacting liquid, and also on the mutual interactions among the permeants. Therefore, a study on membrane swelling at different mass fractions of feed plays an important role in understanding the behavior of membranes in the PV process.

To study the effects of feed composition and silica precursors on membrane swelling, the percent degree of swelling of all of the membranes was plotted at different mass fraction of water in the feed at 303 K as shown in Figure 3. It is found that the degree of swelling was increased almost linearly for all of the membranes with increasing the mass fraction of water in the feed. This was attributed to a strong interaction occurring between the water molecules and the membrane, owing to the presence of  $-\text{NH}_3^+$  and  $-\text{OH}$  groups in the membrane matrix. The interaction becomes prominent with increasing the concentration of water. This is expected as water is more polar than those of alcohols. When the polymer matrices are incorporated with silica precursors, the degree of swelling was correspondingly increased, and this was predominant with increasing the content of GPTMS. This is because of the increased number of  $-\text{OH}$  groups in the matrix.

**Effects of Feed Composition and Silica Precursors on Pervaporation.** Figure 4 shows the effect of feed composition on the total permeation flux for all of the membranes at 303 K. It is found that the total permeation flux was increased almost linearly for all of the membranes with increasing the mass fraction of water in the feed. This is due to an increase of both driving force as well as the degree of membrane swelling. The

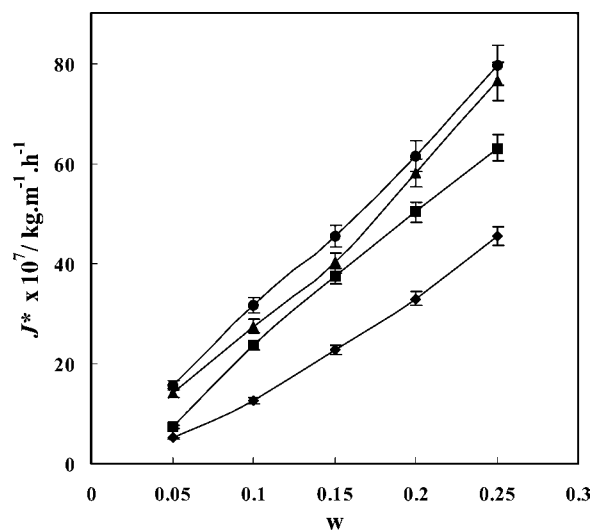


**Figure 4.** Variation of thickness-normalized total flux ( $J^*$ ) with different mass fractions of water ( $w$ ) in the feed for hybrid membranes:  $\blacklozenge$ , (M-1) 100/0 mass ratio;  $\blacksquare$ , (M-2) 75/25 mass ratio;  $\blacktriangle$ , (M-3) 50/50 mass ratio;  $\bullet$ , (M-4) 25/75 mass ratio of TEOS/GPTMS.

driving force is expected because of the increased amount of water in the feed. However, the dependence of the degree of swelling on the the transport of water was ascertained by plotting flux as a function of fugacity, which was nonlinear in nature. Similarly, the total permeation flux was increased with increasing the mass fraction of GPTMS in the membrane. This was mainly attributed to an increase of hydrophilic character as evidenced by FTIR data and swelling study due to the incorporation of GPTMS and its increased mass fraction in the chitosan matrix. The GPTMS is a modified sol–gel precursor,<sup>32,33</sup> which possesses an organically modified alkoxide moiety. This alkoxide moiety contains an epoxy ring, which is basically highly active, and therefore, the epoxy ring readily opens up and allows the formation of hydroxyl groups. This renders the inorganic sol higher hydrophilicity and, thus, enhances its compatibility with chitosan.

To assess the permeation behavior of individual components, we have plotted the individual fluxes as a function of mass fraction of silica precursors at 0.1 mass fraction of water in the feed, and the data are shown in Figure 5. From the plot, it is clearly observed that the total flux and flux of water are almost overlapping each other up to 0.25 mass fraction of GPTMS (M-3), and then the flux of water was deviated from the total flux when the content of GPTMS was increased beyond 0.5 mass fraction, but still the deviation is insignificant. As a result, the flux of isopropanol was negligibly small. This explicates that membranes developed in the present study are highly selective toward water.

The overall selectivity of a membrane in the PV process is generally explained on the basis of interaction between the membrane and the permeating molecules and the molecular size of the permeating species. Figure 6 displays the effect of water composition on the selectivity of all of the membranes. It is observed that there was a significant decrease in selectivity of all of the membranes with increasing water composition from (0.05 to 0.1) mass fraction. However, this was decreased gradually with further increasing the water composition in the feed. At higher concentrations of water in the feed, the membrane swells greatly and results to plasticized membrane upstream because of establishing strong interaction between the membrane and the water molecules. The resulting plasticized

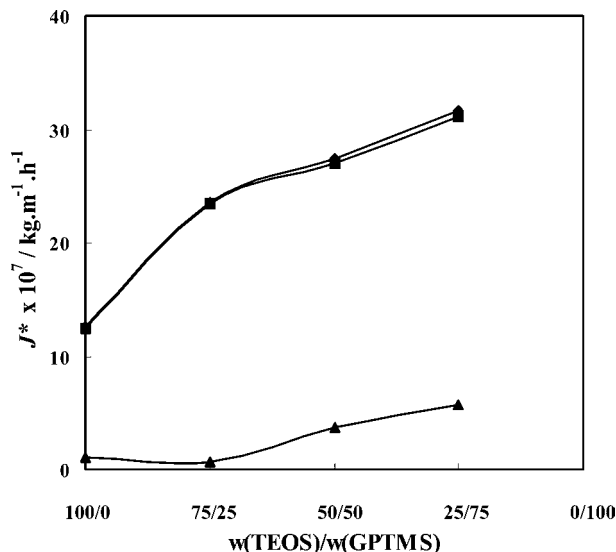


**Figure 5.** Variation of thickness-normalized total flux, ♦; fluxes of water, ■, and isopropanol, ▲, with different mass ratios of TEOS/GPTMS at 0.10 mass fraction of water in the feed.

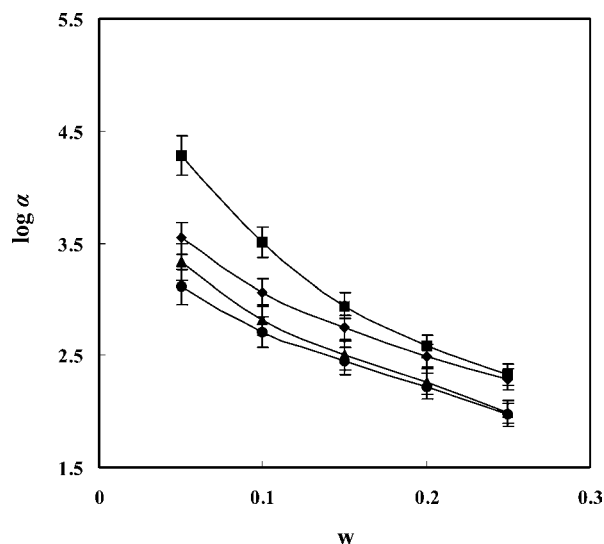


**Figure 6.** Variation of  $\log \alpha$  with different mass fractions of water ( $w$ ) in the feed for hybrid membranes: ♦, (M-1) 100/0 mass ratio; ■, (M-2) 75/25 mass ratio; ▲, (M-3) 50/50 mass ratio; ●, (M-4) 25/75 mass ratio of TEOS/GPTMS.

upstream membrane layer allows some of isopropanol molecules along with selective water molecules, which causes a negative impact on the membranes' selectivity.

On the other hand, the selectivity was increased significantly from membrane M-1 to M-2, and then, it was decreased correspondingly with further increasing the GPTMS content in the membrane (M-3 to M-4). The increasing tendency was attributed to increased cross-linking density and hydrophilic character. However, the further decrease in selectivity from membrane M-3 to M-4 was attributed to increased hydrophilicity and decreased silica content. This was further demonstrated from Figure 7, in which flux and selectivity were plotted as a function of GPTMS content in the membranes at 0.1 mass fraction of water in the feed. Generally, as the packing density of the membranes increases because of either the increase of cross-linking or the incorporation of fillers into the membrane matrix, the permeation flux decreases, and selectivity increases.<sup>34,35</sup> However, in the present study both permeation flux and selectivity were increased simultaneously with increasing

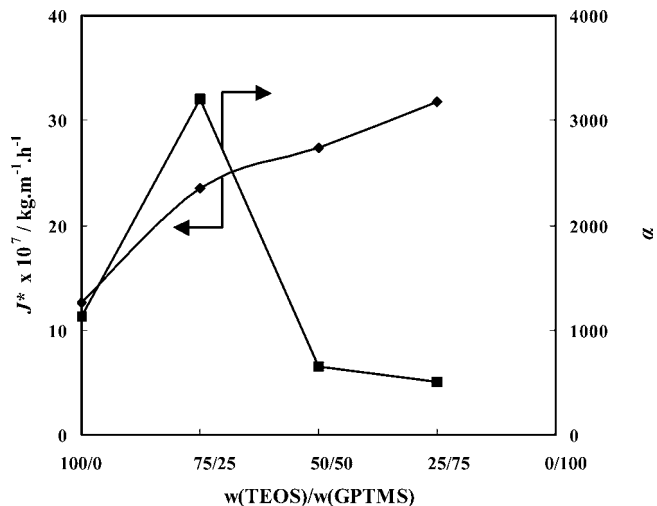


**Figure 7.** Variation of thickness-normalized total flux ( $J^*$ ) and selectivity ( $\alpha$ ) with different mass ratios of TEOS/GPTMS at 0.10 mass fraction of water in the feed.

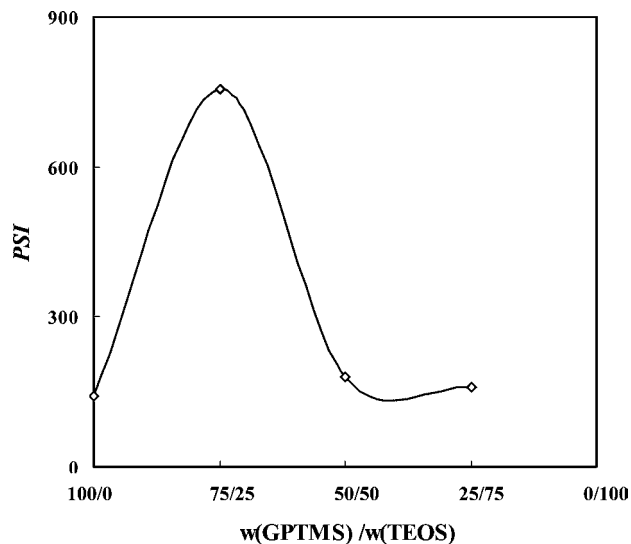


**Figure 8.** Variation of the PV separation index (PSI) with different mass ratios of TEOS/GPTMS at 0.10 mass fraction of water in the feed.

GPTMS content up to 0.25 mass fraction in the membrane. Although a simultaneous increase of both flux and selectivity is uncommon due to a trade-off phenomenon existing between flux and selectivity in the PV process, a significant enhancement of hydrophilicity and cross-linking density has overcome this phenomenon. The enhancement of hydrophilicity and cross-linking was caused by the opening of the epoxy ring in GPTMS. However, when the content of GPTMS was increased beyond 0.25 mass fraction, the selectivity was collapsed. This is due to increased hydrophilicity and decreased silica content.

**Effect of Silica Precursors on Pervaporation Separation Index (PSI).** The PSI is the product of total permeation flux and separation factor, which characterizes the membrane separation ability. This index can be used as a relative guideline for the design of new membranes and also to select a membrane with an optimal combination of flux and selectivity for PV separation processes. Figure 8 shows the variation of PSI as a function of mass fraction of GPTMS at 303 K for 0.1 mass fraction of water in the feed. It is observed that there was a significant enhancement in the PSI values with increasing the GPTMS content from (0 to 0.25) mass fraction in the membrane. As discussed above, this was attributed to the formation of cross-

**Table 1. Comparative Study of PV Performance of Chitosan-Based Membranes Reported in the Literature for the Dehydration of Isopropanol<sup>a</sup>**

membrane	$d$	$T$	$w$	$J$		PSI	ref
	$\mu\text{m}$	K		$\text{kg}\cdot\text{m}^{-2}\cdot\text{h}^{-1}$	$\alpha$		
CS-HPC-10	30	303	0.10	0.110	4277	470	38
CS-HPC-20	30	303	0.10	0.132	11241	148	38
CS-HPC-30	30	303	0.10	0.191	1002	191	38
CS-HPC-40	30	303	0.10	0.226	453	102	38
CS cross-linked with HMDI		303	0.05	0.082	1964	161	39
CS/PTFE	100	343	0.30	1.730	775	1339	40
CS cross-linked with TDI	50	303	0.084	0.079	472	37	41
CS/GPTMS (CSHM-5)	12	343	0.30	1.730	694	1199	26
CMCS/PS composite cross-linked with GA	40	318	0.125	0.039	3239	126	42
CS/PVA-20 cross-linked with USF	35 to 40	303	0.10	0.113	17991	2033	43
CS/PVA-40 cross-linked with USF	35 to 40	303	0.10	0.149	8562	1276	43
CS/PVA-60 cross-linked with USF	35 to 40	303	0.10	0.214	6419	1373	43
CS/silk fibroin (20 mass fraction)	30	323	0.12	0.088			44
CS/silk fibroin (20 mass fraction) cross-linked with GA	30	323	0.12	0.103			44
PVA/TEOS modified with CS (5 mass fraction)	45	303	0.10	0.216	1116	241	45
PVA/TEOS modified with CS (10 mass fraction)	45	303	0.10	0.234	1791	419	45
PVA/TEOS modified with CS (15 mass fraction)	45	303	0.10	0.239	2991	715	45
CS/NaY zeolite (10 mass fraction)	40	303	0.10	0.620	246	152	37
CS/NaY zeolite (20 mass fraction)	40	303	0.10	0.794	345	273	37
CS/NaY zeolite (30 mass fraction)	40	303	0.10	0.976	452	440	37
CS/NaY zeolite (40 mass fraction)	40	303	0.10	1.230	603	740	37
CS/HMDACS (10 mass fraction)	40	303	0.10	0.534	491	262	36
CS/HMDACS (20 mass fraction)	40	303	0.10	0.440	705	310	36
CS/HMDACS (30 mass fraction)	40	303	0.10	0.421	1062	447	36
CS/HMDACS (40 mass fraction)	40	303	0.10	0.342	2423	828	36
CS/TiO <sub>2</sub> (10 mass fraction)	40	303	0.10	0.667	1315	876	22
CS/TiO <sub>2</sub> (20 mass fraction)	40	303	0.10	0.904	1906	1722	22
CS/TiO <sub>2</sub> (30 mass fraction)	40	303	0.10	1.117	2491	2781	22
CS/TiO <sub>2</sub> (40 mass fraction)	40	303	0.10	1.524	4728	7204	22
CS/TEOS-GPTMS (M-1)	40	303	0.10	0.316	1130	356	present work
CS/TEOS-GPTMS (M-2)	40	303	0.10	0.590	3205	1890	present work
CS/TEOS-GPTMS (M-3)	40	303	0.10	0.685	653	446	present work
CS/TEOS-GPTMS (M-4)	40	303	0.10	0.793	502	397	present work

<sup>a</sup>  $d$ , thickness;  $T$ , temperature;  $w$ , mass fractions of water in the feed;  $J$ , flux;  $\alpha$ , selectivity; M-1, 100/0 mass ratio; M-2, 75/25 mass ratio; M-3, 50/50 mass ratio; M-4, 25/75 mass ratio of TEOS/GPTMS. CS: chitosan; GPTMS:  $\gamma$ -glycidoxypropyltrimethoxysilane; TEOS: tetraethoxysilane; PTFE: poly(tetrafluoroethylene); PS: polysulfone; HMDACS: hexamethylene 1,6-di(aminocarboxysulfonate); USF: urea formaldehyde/sulfuric acid; CSHM: chitosan silica hybrid membrane; HPC: hydroxylpropyl cellulose; CMCS: carboxymethyl chitosan; TDI: toluene-2,4-diisocyanate; PVA: poly(vinyl alcohol); GA: glutaraldehyde.

links and enhanced hydrophilic character. A further increase of GPTMS from (0.25 to 0.5) mass fraction reduces the selectivity from 18 981 to 2134, which was responsible for the further decrease in PSI values.

**Comparison of PV Performance of Chitosan-Based Membranes.** The flux and selectivity including the data of PSI of the chitosan-based membranes for the separation of water–isopropanol mixtures are presented in Table 1 and the tabulated performance data shown graphically in the logarithmic plot in Figure 9. It is observed that hybrid membranes developed in the present study exhibited better permeation flux compared to most of the chitosan-based membranes reported in the literature.<sup>22,26,36–45</sup> The homogeneous membranes (CS/GPTMS and CS/PTFE) reported by Liu et al.<sup>26,40</sup> showed higher permeation flux compared to the membranes developed here. But, it is not surprising, since they have carried out the experiment at a higher temperature (343 K) with a higher mass fraction of water (0.30) in the feed. Similarly, the heterogeneous membranes such as CS/NaY zeolite<sup>37</sup> and CS/TiO<sub>2</sub><sup>22</sup> reported by our own group demonstrated better permeation flux than those of the membranes developed here. This is expected because both NaY zeolite and TiO<sub>2</sub> are known to increase the hydrophilicity of the membranes. Unfortunately, these membranes exhibit poor mechanical strength due to their heterogeneous nature. With regard to selectivity, the hybrid membranes developed here demonstrated an excellent selectivity com-

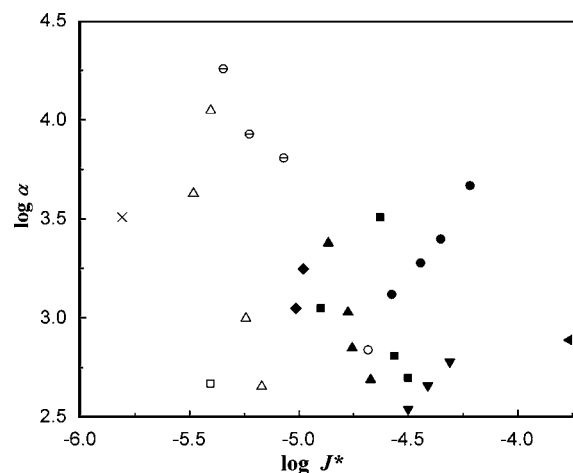


**Figure 9.** Graphical representation of membrane performance data presented in Table 1:  $\alpha$ , selectivity;  $J^*$ , thickness-normalized flux;  $\Delta$ , CS-HPC; solid left-pointing triangle, CS/PTFE;  $\square$ , CS cross-linked with TDI;  $\circ$ , CS/GPTMS (CSHM-5);  $\times$ , CMCS/PS composite cross-linked with GA;  $\ominus$ , CS/PVA cross-linked with USF;  $\blacklozenge$ , PVA/TEOS;  $\blacktriangledown$ , CS/NaY zeolite;  $\blacktriangle$ , CS/HMDACS;  $\bullet$ , CS/TiO<sub>2</sub>;  $\blacksquare$ , CS/TEOS-GPTMS.

pared to all other homogeneous membranes. However, the selectivity of the heterogeneous membranes is comparable. Similarly, the data of PSI also support the above statement. Hence, it can be concluded that the hybrid membranes developed here are better candidates for the dehydration of isopropanol.

**Table 2. PV Flux ( $J$ ) and Separation Selectivity ( $\alpha$ ) for Different Membranes at Different Temperatures for 0.10 Mass Fractions of Water in the Feed ( $w$ )<sup>a</sup>**

T/K	$10^2 J/\text{kg}\cdot\text{m}^{-2}\cdot\text{h}^{-1}$				$\alpha$			
	M-1	M-2	M-3	M-4	M-1	M-2	M-3	M-4
303	3.16	5.90	6.85	7.93	1130	3205	653	502
	$\pm 0.10$	$\pm 0.21$	$\pm 0.28$	$\pm 0.36$	$\pm 36$	$\pm 115$	$\pm 26$	$\pm 23$
313	4.14	6.89	7.82	8.83	802	1038	455	393
	$\pm 0.13$	$\pm 0.25$	$\pm 0.33$	$\pm 0.41$	$\pm 26$	$\pm 38$	$\pm 19$	$\pm 18$
323	5.75	8.50	9.45	10.44	583	747	318	283
	$\pm 0.19$	$\pm 0.33$	$\pm 0.42$	$\pm 0.51$	$\pm 19$	$\pm 29$	$\pm 14$	$\pm 13$

<sup>a</sup> M-1, 100/0 mass ratio; M-2, 75/25 mass ratio; M-3, 50/50 mass ratio; M-4, 25/75 mass ratio of TEOS/GPTMS.

**Effect of Temperature on Membrane Performance.** The effect of operating temperature on the PV performance for water–isopropanol mixtures was studied for all of the membranes at 0.1 mass fraction of water in the feed, and resulting values are presented in Table 2. It is observed that the permeation rate was increased from (303 to 323) K for all of the membranes, while decreasing the separation selectivity. Generally, this happens because of two reasons. First, as the temperature increases the vapor pressure difference between the upstream and the downstream side of the membranes increases, and this in turn enhances the transport of driving force. Second, an increase of temperature promotes the thermal motion of polymer chain segments, creating more free volume in the polymer matrix. However, in the present study, the latter reason is ruled out since the experiments were performed well below the glass transition temperature of chitosan. Therefore, the driving force played a major role in transporting the associated molecules along with the selective permeants. This results to an increase of total permeation flux while suppressing the selectivity. Thus, the temperature dependence of permeation has prompted us to estimate the activation energies for permeation using the Arrhenius type equation:<sup>46</sup>

$$J = J_0 \exp\left(\frac{-E_x}{RT}\right) \quad (5)$$

where  $J$  is the permeation per unit area and  $J_0$  is a constant representing pre-exponential factor.  $E$  represents the activation energy for permeation, subscript  $x$  stands for water or isopropanol, and  $RT$  is the usual energy term. As the feed temperature increases, the vapor pressure in the feed compartment also increases, but the vapor pressure at the permeate side is not affected. This leads to an increase of driving force with increasing the temperature.

Arrhenius plot of  $\log J$  versus temperature is shown in Figure 10. A linear behavior was observed, suggesting that permeability follows an Arrhenius trend. From the least-squares fits of these linear plots, the activation energies for total permeation ( $E_p$ ) for all of the membranes were estimated. Similarly, we have also estimated the activation energies for permeation of water ( $E_{pw}$ ) and isopropanol ( $E_{pIPA}$ ), but the plots are not given to avoid the crowdedness. The values thus obtained are presented in Table 3.

From Table 3, it can be seen that the apparent activation energy values for water permeation ( $E_{pw}$ ) are more than three times lower than those of isopropanol ( $E_{pIPA}$ ) particularly for GPTMS incorporated membranes (M-2 to M-4), suggesting that membranes developed here have higher separation efficiency toward water. The activation energy values of water permeation ( $E_{pw}$ ) and total permeation ( $E_p$ ) are almost close to each other, signifying that coupled-transport of both water and isopropanol

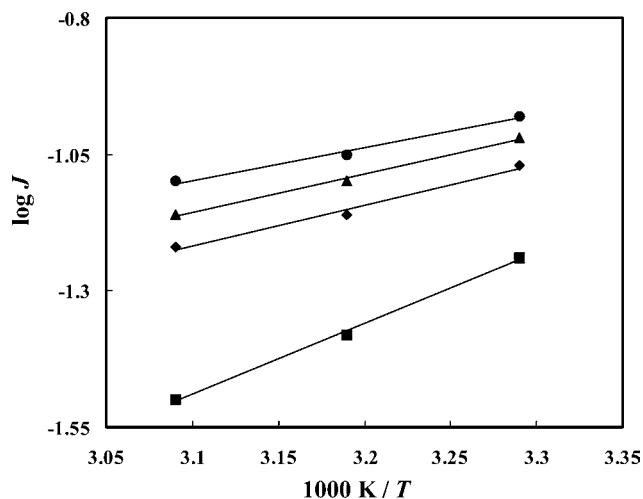


**Figure 10.** Variation of  $\log J$  with temperature for hybrid membranes at 0.10 mass fraction of water in the feed:  $\diamond$ , (M-1) 100/0 mass ratio;  $\blacksquare$ , (M-2) 75/25 mass ratio;  $\blacktriangle$ , (M-3) 50/50 mass ratio;  $\bullet$ , (M-4) 25/75 mass ratio of TEOS/GPTMS.

**Table 3. Arrhenius Activation Parameters for Total Permeation ( $E_p$ ), Permeation of Water ( $E_{pw}$ ), and Permeation of Isopropanol ( $E_{pIPA}$ )<sup>a</sup>**

parameters	M-1	M-2	M-3	M-4
$E_p/\text{kJ}\cdot\text{mol}^{-1}$	24.50	14.85	13.07	11.18
$E_{pw}/\text{kJ}\cdot\text{mol}^{-1}$	24.19	14.48	12.49	10.63
$E_{pIPA}/\text{kJ}\cdot\text{mol}^{-1}$	51.06	74.08	41.75	33.85

<sup>a</sup> M-1, 100/0 mass ratio; M-2, 75/25 mass ratio; M-3, 50/50 mass ratio; M-4, 25/75 mass ratio of TEOS/GPTMS.

is minimal as due to higher selective nature of membranes. It is further noticed that, as the GPTMS content was increased from membrane M-2 to M-4, the activation energy values of  $E_p$  were also decreased. This is expected because of increased hydrophilicity with increasing the content of GPTMS in the membrane matrix, which obviously reduces the energy required for transport of selective permeants. The estimated  $E_p$  values ranged between (24.50 and 11.18)  $\text{kJ}\cdot\text{mol}^{-1}$ .

## Conclusions

Using a sol–gel technique, hybrid membranes were prepared using chitosan and mixed silica precursors. The membranes were employed to separate water–isopropanol mixtures at (303, 313, and 323) K. An increase of GPTMS content results to a simultaneous increase of both permeation flux and selectivity, although it was restricted to only 0.25 mass fraction of GPTMS. This was explained on the basis of the enhancement of hydrophilic character and increased cross-linking density. However, the decrease in selectivity beyond 0.25 mass fraction of GPTMS was attributed to increased hydrophilicity and decreased silica yield. Experimental data also reveal that the total flux and water flux are overlapping each other except for the membrane M-4, suggesting that the developed membranes are highly selective toward water. The PV separation index data clearly indicated that the membrane with 0.25 mass fraction of GPTMS showed an excellent PV performance. Therefore, the membrane containing 0.25 mass fraction of GPTMS showed the highest separation selectivity of 18 981 with a thickness-normalized flux of  $7.45\cdot 10^{-7} \text{ kg}\cdot\text{m}^{-1}\cdot\text{h}^{-1}$  at 303 K for 0.05 mass fraction of water in the feed. With an increase in temperature, the permeation flux was increased while decreasing the selectivity, and this was attributed to decreased interaction between the permeants. The hybrid membranes containing

higher amount of GPTMS showed significantly lower activation energy values, indicating that the permeants consumed less energy as a result of increased hydrophilicity. The membranes showed lower activation energy values for water permeation ( $E_{pw}$ ) than that of isopropanol permeation ( $E_{pIPA}$ ), signifying that the membranes developed here demonstrated excellent separation efficiency toward water.

### Acknowledgment

Authors sincerely thank the Department of Physics, Indian Institute of Science, Bangalore for extending wide-angle X-ray diffraction facility.

### Supporting Information Available:

Experimental section in regard to FTIR, WAXD, SEM, and TGA. Results and discussion on membrane characterization and its corresponding figures. This material is available free of charge via the Internet at <http://pubs.acs.org>.

### Literature Cited

- Mammeri, F.; Bourhis, E. L.; Rozes, L.; Sanchez, C. Mechanical Properties of Hybrid Organic-Inorganic Materials. *J. Mater. Chem.* **2005**, *15*, 3787–3811.
- Matejka, L.; Dukh, O.; Meissner, B.; Hlavata, D.; Brus, J.; Strachota, A. Block Copolymer Organic-Inorganic Networks: Formation and Structure Ordering. *Macromolecules* **2004**, *36*, 7977–7985.
- Gomez-Romero, P. Hybrid Organic-Inorganic Materials - In Search of Synergic Activity. *Adv. Mater.* **2001**, *13*, 163–174.
- Gomez-Romero, P.; Sanchez, C. *Functional Hybrid Materials*; Wiley VCH: Weinheim, 2004.
- Sanchez, C.; Lebeau, B.; Chaput, F.; Boilot, J. P. Optical Properties of Functional Hybrid Organic-Inorganic Nanocomposites. *Adv. Mater.* **2003**, *15*, 1969–1994.
- Ricciaedi, R.; Auriemma, F.; Rosa, C. D.; Laupretre, F. X-ray Diffraction Analysis of Poly(vinyl alcohol) Hydrogels, Obtained by Freezing and Thawing Techniques. *Macromolecules* **2004**, *37*, 1921–1927.
- Gomez-Romero, P.; Sanchez, C. Hybrid Materials. Functional Properties. From Maya Blue to 21st Century Materials. *New J. Chem.* **2005**, *29*, 57–58.
- Sanchez, C.; Ribot, F. Design of Hybrid Organic-Inorganic Materials Synthesized via Sol-Gel Chemistry. *New J. Chem.* **1994**, *18*, 1007–1047.
- Shea, K. J.; Loy, D. A. Bridged Polysilsesquioxanes. Molecular Engineered Hybrid Organic-Inorganic Materials. *Chem. Mater.* **2001**, *13*, 3306–3319.
- Schubert, U. Silica-Based and Transition Metal-Based Inorganic-Organic Hybrid Materials - A Comparison. *J. Sol-Gel Sci. Technol.* **2003**, *26*, 47–55.
- Judeinstein, P.; Sanchez, C. Hybrid Organic-Inorganic Materials, A Land of Multidisciplinarity. *J. Mater. Chem.* **1996**, *6*, 511–525.
- Sanchez, C.; Lebeau, B.; Ribot, F.; In, M. Molecular Design of Sol-Gel Derived Hybrid Organic-Inorganic Nano-Composites. *J. Sol-Gel Sci. Technol.* **2000**, *19*, 31–38.
- Innocenzi, P.; Esposito, M.; Maddalena, A. Mechanical Properties of 3-Glycidoxypropyltrimethoxysilane Based Hybrid Organic-Inorganic Materials. *J. Sol-Gel Sci. Technol.* **2001**, *20*, 293–301.
- Chen, J. H.; Liu, Q. L.; Zhang, X. H.; Zhang, Q. G. Pervaporation and Characterization of Chitosan Membranes Crosslinked by 3-Aminopropyltriethoxysilane. *J. Membr. Sci.* **2007**, *292*, 125–132.
- Peng, F.; Lu, L.; Sun, H.; Pan, F.; Jiang, Z. Organic-Inorganic Hybrid Membranes with Simultaneously Enhanced Flux and Selectivity. *Ind. Eng. Chem. Res.* **2007**, *46*, 2544–2549.
- Uragami, T.; Yanagisawa, S.; Miyata, T. Water/Ethanol Selectivity of New Organic-Inorganic Hybrid Membranes Fabricated from Poly(vinyl alcohol) and an Organosilane. *Macromol. Chem. Phys.* **2007**, *208*, 756–764.
- Castricum, H. L.; Kreiter, R.; Veen, H. M. V.; Blank, D. H. A.; Vente, J. F.; Elshof, J. E. T. High-Performance Hybrid Pervaporation Membranes with Superior Hydrothermal and Acid Stability. *J. Membr. Sci.* **2008**, *324*, 111–118.
- Zhang, Q. G.; Liu, Q. L.; Jiang, Z. Y.; Chen, Y. Anti-Trade-Off in Dehydration of Ethanol by Novel PVA/APTEOS Hybrid Membranes. *J. Membr. Sci.* **2007**, *287*, 237–245.
- Uragami, T.; Katayama, T.; Miyata, T.; Tamura, H.; Shiraiwa, T.; Higuchi, A. Dehydration of an Ethanol/Water Azeotrope by Novel Organic-Inorganic Hybrid Membrane Based on Quaternized Chitosan and Tetraethoxysilane. *Biomacromolecules* **2004**, *5*, 1567–1574.
- Uragami, T.; Okazaki, K.; Matsugi, H.; Miyata, T. Structure and Permeation Characteristics of an Aqueous Ethanol Solution of Organic-Inorganic Hybrid Membranes Composed of Poly(vinyl alcohol) and Tetraethoxysilane. *Macromolecules* **2002**, *35*, 9156–9163.
- Kariduraganavar, M. Y.; Kulkarni, S. S.; Kittur, A. A. Pervaporation Separation of Water-Acetic Acid Mixtures through Poly(vinyl alcohol)-Silicone Based Hybrid Membranes. *J. Membr. Sci.* **2005**, *246*, 83–93.
- Kariduraganavar, M. Y.; Varghese, J. G.; Choudhari, S. K.; Olley, R. H. Organic-Inorganic Hybrid Membranes: Solving the Trade-Off Phenomenon Between Permeation Flux and Selectivity in Pervaporation. *Ind. Eng. Chem. Res.* **2009**, *48*, 4002–4013.
- Kalyani, S.; Smitha, B.; Sridhar, S.; Krishnaiah, A. Pervaporation Separation of Ethanol-Water Mixtures Through Sodium Alginate Membranes. *Desalination* **2008**, *229*, 68–81.
- Silva, S. S.; Ferreira, R. A. S.; Fu, L.; Carlos, L. D.; Mano, J. F.; Reis, R. L.; Rocha, J. Functional Nanostructured Chitosan-Siloxane Hybrids. *J. Mater. Chem.* **2005**, *15*, 3952–3961.
- Liu, Y. L.; Hsu, C. Y.; Su, Y. H.; Lai, J. Y. Chitosan-Silica Complex Membranes for Sulfonic Acid Functionalized Silica Nanoparticles for Pervaporation Dehydration of Ethanol-Water Solutions. *Biomacromolecules* **2005**, *6*, 368–373.
- Liu, Y. L.; Su, Y. H.; Lee, K. R.; Lai, J. Y. Crosslinked Organic-Inorganic Hybrid Chitosan Membranes for Pervaporation Dehydration of Isopropanol-Water Mixtures with a Long-Term Stability. *J. Membr. Sci.* **2005**, *251*, 233–238.
- Park, S. B.; You, J. O.; Park, H. Y.; Hamm, S. J.; Kim, W. S. A Novel pH-Sensitive Membrane from Chitosan-TEOS IPN; Preparation and its Drug Permeation Characteristics. *Biomaterials* **2001**, *22*, 323–330.
- Hsiue, G. H.; Chen, J. K.; Liu, Y. L. Synthesis and Characterization of Nanocomposite of Polyimide-Silica Hybrid from Non-Aqueous Sol-Gel Process. *J. Appl. Polym. Sci.* **2000**, *76*, 1609–1618.
- Liu, Y. L.; Su, Y. H.; Lai, J. Y. In Situ Crosslinking of Chitosan and Formation of Chitosan-Silica Hybrid Membranes with Using  $\gamma$ -Glycidoxypropyltrimethoxysilane as a Crosslinking Agent. *Polymer* **2004**, *45*, 6831–6837.
- Peng, F.; Lu, L.; Sun, H.; Wang, Y.; Liu, J.; Jiang, Z. Hybrid Organic-Inorganic Membrane: Solving the Trade-Off Between Permeability and Selectivity. *Chem. Mater.* **2005**, *17*, 6790–6796.
- Kariduraganavar, M. Y.; Kittur, A. A.; Kulkarni, S. S.; Ramesh, K. Development of Novel Pervaporation Membranes for the Separation of Water-Isopropanol Mixtures Using Sodium Alginate and NaY Zeolite. *J. Membr. Sci.* **2004**, *238*, 165–175.
- Sarkel, D.; Roy, D.; Bandyopadhyay, M.; Bhattacharya, P. Studies on Separation Characteristics and Pseudo-Equilibrium Relationship in Pervaporation of Benzene-Cyclohexane Mixtures through Composite PVA Membranes on PAN Support. *Sep. Purif. Technol.* **2003**, *30*, 89–96.
- Pandey, L. K.; Saxena, C.; Dubey, V. Modification of poly(vinyl alcohol) Membranes for Pervaporative Separation of Benzene/Cyclohexane Mixtures. *J. Membr. Sci.* **2003**, *227*, 173–182.
- Kittur, A. A.; Kariduraganavar, M. Y.; Toti, U. S.; Ramesh, K.; Aminabhavi, T. M. Pervaporation Separation of Water-Isopropanol Mixtures Using ZSM-5 Zeolite Incorporated Poly(vinyl alcohol) Membranes. *J. Appl. Polym. Sci.* **2003**, *90*, 2441–2448.
- Kulkarni, S. S.; Tambe, S. M.; Kittur, A. A.; Kariduraganavar, M. Y. Preparation of Novel Composite Membranes for the Pervaporation Separation of Water-Acetic Acid Mixtures. *J. Membr. Sci.* **2006**, *285*, 420–431.
- Choudhari, S. K.; Kittur, A. A.; Kulkarni, S. S.; Kariduraganavar, M. Y. Development of Novel Blocked Diisocyanate Crosslinked Chitosan Membranes for Pervaporation Separation of Water-Isopropanol Mixtures. *J. Membr. Sci.* **2007**, *302*, 197–206.
- Kittur, A. A.; Kulkarni, S. S.; Aralaguppi, M. I.; Kariduraganavar, M. Y. Preparation and Characterization of Novel Pervaporation Membranes for the Separation of Water-Isopropanol Mixtures Using Chitosan and NaY Zeolite. *J. Membr. Sci.* **2005**, *247*, 75–86.
- Veerapur, R. S.; Gudasi, K. B.; Aminabhavi, T. M. Pervaporation Dehydration of Isopropanol Using Blend Membranes of Chitosan and Hydroxypropyl Cellulose. *J. Membr. Sci.* **2007**, *304*, 102–111.
- Ghazali, M.; Nawawi, M.; Huang, R. Y. M. Pervaporation Dehydration of Isopropanol with Chitosan Membranes. *J. Membr. Sci.* **1997**, *124*, 53–62.
- Liu, Y. L.; Yu, C. H.; Lee, K. R.; Lai, J. Y. Chitosan/Poly(tetrafluoroethylene) Composite Membranes Using in Pervaporation Dehydration Processes. *J. Membr. Sci.* **2007**, *287*, 230–236.
- Devi, A. D.; Smitha, B.; Sridhar, S.; Aminabhavi, T. M. Pervaporation Separation of Isopropanol/Water Mixtures through Crosslinked Chitosan Membranes. *J. Membr. Sci.* **2005**, *262*, 91–99.
- Shen, J. N.; Wu, L. G.; Qiu, J. H.; Gao, C. J. Pervaporation Separation of Water/Isopropanol Mixtures Through Crosslinked Carboxymethyl



- Chitosan/Polysulfone Hollow-Fiber Composite Membranes. *J. Appl. Polym. Sci.* **2007**, *103*, 1959–1965.
- (43) Rao, K.; Subha, M. C. S.; Sairam, M.; Mallikarjuna, N. N.; Aminabhavi, T. M. Blend Membranes of Chitosan and Poly(vinyl alcohol) in Pervaporation Dehydration of Isopropanol and Tetrahydrofuran. *J. Appl. Polym. Sci.* **2007**, *103*, 1918–1926.
- (44) Chen, X.; Li, W.; Shao, Z.; Zhong, W.; Yu, T. Separation of Alcohol-Water Mixture by Pervaporation Through a Novel Natural Polymer Blend Membrane-Chitosan/Silk Fibroin Blend Membrane. *J. Appl. Polym. Sci.* **1999**, *23*, 975–980.
- (45) Kulkarni, S. S.; Tambe, S. M.; Kittur, A. A.; Kariduraganavar, M. Y. Modification of Tetraethylorthosilicate Crosslinked Poly(vinyl alcohol) Membrane Using Chitosan and its Application to the Pervaporation Separation of Water-Isopropanol Mixtures. *J. Appl. Polym. Sci.* **2006**, *99*, 1380–1389.
- (46) Huang, R. Y. M.; Yeom, C. K. Pervaporation Separation of Aqueous Mixtures Using Crosslinked Poly(vinyl alcohol) Membranes. III. Permeation of Acetic Acid-Water Mixtures. *J. Membr. Sci.* **1991**, *58*, 33–47.

Received for review May 5, 2009. Accepted April 17, 2010. One of the authors (J.G.V.) wishes to acknowledge the UGC, New Delhi for awarding the Research Fellowship under meritorious category.

JE9003993